PCCP

Accepted Manuscript

ROYAL SOCIETY OF CHEMISTRY

www.rsc.org/pccp

PCCP

Paper

Application-oriented computational studies on a series of D-π-A structured porphyrin sensitizers with different electron-donor groups

Received 00th January 20xx,
Accepted 00th January 20xx

DOI: 10.1039/x0xx00000x

www.rsc.org/

Chencheng Fan,[ab] Bao Zhang,*[a] Yuanchao Li,[a] Yuxia Liang,[a] Xiaodong Xue[a] and Yaqing Feng*[ab]

A series of D-π-A zinc porphyrin sensitizers **Dye1**-**Dye6** bearing a substituted iminodibenzyl group at the porphyrin meso position, which is expected to have different electron-donating abilities were designed. Theoretical studies were performed to examine the photovoltaic properties of these molecules in dye-sensitized solar cells (DSSCs). In particular, the important concepts, Fukui function and extended condensed Fukui function are employed to describe the electron-donating abilities accurately in a quantitative level. The Tangui Le Bahers's model was adopted to analyze charge transfer (CT) during electron transition. The correlation between the electron donating abilities of the derived iminodibenzyl group and CT was built to evaluate the cell performance based on sensitizers **Dye1**-**Dye6**. The theoretical studies showed that porphyrins **Dye1**-**Dye3** bearing an extremely strong electron-donating group (EDG) would fail in the generation of photocurrent in the closed circuit when applied in DSSCs due to the higher level of the HOMO energy than the redox potential of the redox couple (I^- / I_3^-). The one with a weaker EDG (**Dye4**) is expected to show better photovoltaic performance than porphyrin **IDB** with an unsubstituted iminodibenzyl group. The study demonstrated a reliable method involving the employment of Fukui Function, extended condensed Fukui Function and Tangui Le Bahers' model for the evaluation of the newly designed D-π-A type porphyrin sensitizers for use in DSSCs, and as guidance for the future molecular design.

1. Introduction

Dye-sensitized solar cells (DSSCs) have been widely regarded as a promising candidate for new generation photovoltaics to provide electricity since O'Regan and Gräzel published their pioneering work in 1991.[1] According to the principle of DSSC, when a DSSC is illuminated with light, the electrons in the ground state of the dye are energized to the higher-energy excited states. The excited electrons are injected into the TiO_2 conduction band (CB) and the oxidized dye sensitizers are regenerated by taking electrons from the redox couple in the electrolyte. Therefore, as a key component in DSSCs, dye molecules play an important role in determining the corresponding cell performance.[2,3]

Specifically, for dye excitation, Gouterman[4] thought that it mainly involved the excitations among HOMO-1, HOMO, LUMO and LUMO+1. The photo-excited dyes may decay to the ground state. A long lifetime of the excited electron is favorable for the efficient electron injection, which can lead to high open-circuit voltage (V_{oc}).[5] The recombination reactions between the dye cation and the injected electrons as well as between the electrolyte and the excited electrons are the principal side reactions that occur inside the cell, leading to the loss of photo-electrons.

It is well known that a good alignment of energy level is crucial for cell performance. In order to enhance the light-harvesting ability and increase cell performance, one effective way is to narrow HOMO-LUMO gap by extending the π-conjugation of the molecules. However, the LUMO of the excited state has to lie above the bottom edge of the conduction band of the semiconductor so that injection of electrons into the CB is thermodynamically favorable. The HOMO of the photo-oxidized dyes has to be below the redox potential of the redox couple so that dyes can be regenerated by taking electrons from the redox couple.[6,7]

At present, the "push-pull" type molecules which are made up of electron-donor groups (EDGs) and electron-withdrawing groups (EWGs), connected with π-conjugated spacers (π-bridges) are quite popular for the fabrication of high performance cell. Porphyrin derivatives have drawn considerable attention for use as sensitizers in DSSCs due to their vital roles in natural photosynthetic systems and strong absorption in the visible region, as well as readily tunable optical, photophysical and electrochemical properties by peripheral substitutions.[3,8,9] For example, in 2014, Yella[10] synthesized a "push-pull" type zinc porphyrin dye (**SM315**) featuring a D-π-A structure, based on which the solar cell exhibits remarkably high power conversion efficiency (η) value

[a] School of Chemical Engineering and Technology, Tianjin University, Tianjin, China. E-mail: baozhang@tju.edu.cn; yqfeng@tju.edu.cn.
[b] Collaborative Innovation Center of Chemical Science and Engineering, Tianjin 300072.

of up to 13% using a cobalt-based redox electrolyte. By using a co-sensitization strategy, the η value reached 14.7%,[11] which is a new milestone achieved in the DSSCs field.

In the design of efficient sensitizers for use in DSSCs, it is vital to introduce suitable donor and acceptor groups to modulate molecular energy levels.[12] For example, Xie[13, 14] designed and synthesized porphyrin sensitizers with the EDGs or EWGs systematically varied and investigated their effects on the cell performance. Recently, in our continuous efforts to develop high performance porphyrin sensitizers for use in DSSCs, we synthesized three D-π-A zinc porphyrin molecules bearing different diarylamino groups such as diphenylamine (DPA), iminodibenzyl (IDB) and iminostibene (ISB) as the electron pushing group, and benzo cyanoacrylic acid as π-spacer and the electron acceptor (figure 1).[15] The corresponding cell performances were measured and the molecules were further investigated by means of density functional theory (DFT) calculations and time-dependent functional theory (TD-DFT) calculation. It was shown that best cell performance is achieved by porphyrin **IDB**-sensitized solar cell. [15] By further comparing the computational results with experimental ones[15], we speculate that the porphyrins with stronger EDGs have better cell performance. Thus, on the basis of the structure of the best performance porphyrin (**IDB**), we designed a series of new porphyrins. The electron-donating abilities of the meso-diarylamino group (iminodibenzyl) vary distinctly by introducing either a strong or medium EDG or a EWG to the two benzo rings of the iminodibenzyl substituent para to the amino atom. Compared to porphyrin **IDB**, those porphyrins containing diphenyl/dialkylamino group (**Dye1** and **Dye2**), alkoxyl chain (**Dye3**) or alkyl group (**Dye4**) in the iminodibenzyl substituent are expected to have stronger electron-pushing abilities at the porphyrin meso position, which should facilitate the intramolecular transfer of the photo-generated electrons to the acceptor via π bridge, and to a certain extent enhance the performance of the corresponding porphyrin-based DSSCs. On the other hand, those with electron-drawing substituents present in the iminodibenzyl group such as fluorine atoms (**Dye5**) or cyano groups (**Dye6**) should see a decrease in the cell performance due to the smaller electron-pushing abilities of the derived iminodibenzyl group. In this study, the reliability of the computational method including the employment of the functions and basis sets during the computation was first analyzed based on our previous experimental studies on porphyrins **DPA**, **IDB** and **ISB**, which then can be used to evaluate the performance of the newly designed porphyrin sensitizers **dye1**-**dye6**. The definitions of condensed Fukui function were extended to evaluate the electron donating abilities of the diarylamino groups accurately in a quantitative level. The Tangui Le Bahers's model was adopted to analyze charge transfer (CT) during electron transition. The correlation between the electron donating abilities of EDG and CT was built to evaluate the photovoltaic properties of **dye1**-**dye6** in DSSCs. Interestingly, based on theoretical studies porphyrins bearing a strong EDG failed in generation of photocurrent in the closed circuit when applied in DSSCs, since the HOMO energy level is higher than the redox potential of the redox couple (I^- / I_3^-). The one with a weaker EDG (**Dye4**) is expected to show better photovoltaic performance than porphyrin **IDB** with an unsubstituted iminodibenzyl group. The employment of Fukui Function, extended condensed Fukui Function and Tangui Le Bahers' model provided a method for the evaluation of the newly designed D-π-A type porphyrin sensitizers for use in DSSCs, and as a guidance for the future molecular design.

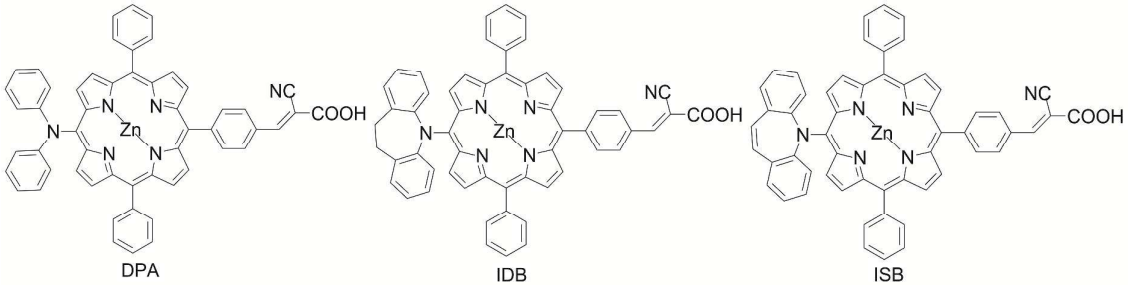

Figure 1 Molecular structures **DPA**, **IDB**, **ISB**

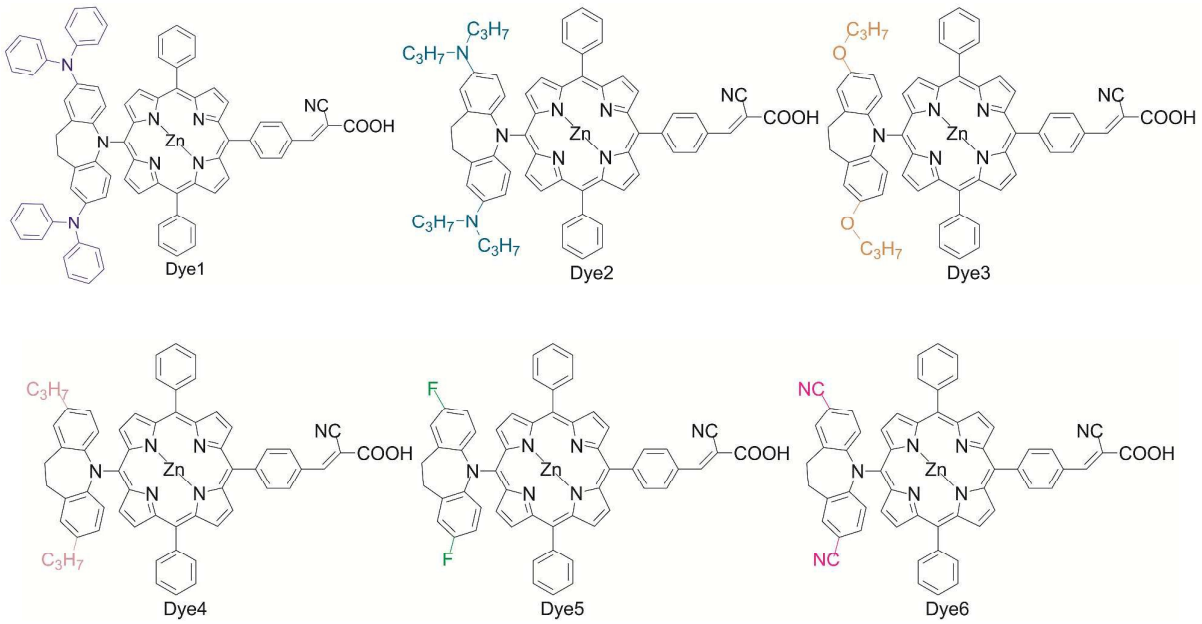

Figure 2 Newly designed Molecular structures **Dye1**-**Dye6**

2. Methodology

2.1 Parameters evaluating sensitizers

As is well known, the overall η, which is the most important measurement index for a solar cell is given by the photocurrent density measured at short-circuit (J_{sc}), the open-circuit photovoltage (V_{oc}), the fill factor of the cell (FF), and the intensity of the incident light (P_{in}),

$$\eta = \frac{J_{sc}V_{oc}FF}{P_{in}} \quad (1)$$

2.2 Frontier Molecular Orbital

According to the frontier molecular orbital (FMO) theory,[16] many properties of molecules are determined by the frontier molecular orbitals, such as the highest occupied molecular orbital (HOMO) and the lowest unoccupied molecular orbital (LUMO) as well as HOMO-1 orbital, LUMO+1 orbital and so on.

The FMO theory is easy to understand and visualize. However it is not accurate enough when evaluating the electron donating abilities in a quantitative level. So we adopt the important concepts, namely Fukui function and condensed Fukui function to describe the electron donating abilities accurately in a quantitative level.

2.3 Fukui Function and Condensed Fukui Function

As an important concept in conceptual density functional theory, Fukui function has been widely used in the prediction of the reactive site. Fukui function is defined as: [17]

$$\boldsymbol{f(r)} = \left(\frac{\partial \rho(\boldsymbol{r})}{\partial N}\right)_{v} \quad (2)$$

where N is number of electrons in the present system and the constant term v in the partial derivative is external potential. Generally the external potential only comes from nuclear charges, and thus v can be seen as nuclear coordinates for isolated chemical system. The partial derivative cannot be directly evaluated due to the discontinuity when N is an integer. To resolve this difficulty, Fukui function is defined using one-sided derivatives.[18]

Nucleophilic attack:

$$\boldsymbol{f^{+}(r)} = \left(\frac{\partial \boldsymbol{\rho(r)}}{\partial \boldsymbol{N}}\right)_{v}^{+} = \underbrace{\boldsymbol{lim}}_{\boldsymbol{\varepsilon \to 0^{+}}} \frac{\boldsymbol{\rho_{N+\varepsilon}(r) - \rho_{N}(r)}}{\boldsymbol{\varepsilon}}$$
$$= \boldsymbol{\rho_{N+1}(r) - \rho_{N}(r) \approx \rho^{LUMO}(r)} \quad (3)$$

Electrophilic attack:

$$\boldsymbol{f^{-}(r)} = \left(\frac{\partial \boldsymbol{\rho(r)}}{\partial \boldsymbol{N}}\right)_{v}^{-} = \underbrace{\boldsymbol{lim}}_{\boldsymbol{\varepsilon \to 0^{+}}} \frac{\boldsymbol{\rho_{N}(r) - \rho_{N-\varepsilon}(r)}}{\boldsymbol{\varepsilon}}$$
$$= \boldsymbol{\rho_{N}(r) - \rho_{N-1}(r) \approx \rho^{HOMO}(r)} \quad (4)$$

Radical attack:

$$\boldsymbol{f^{0}(r)} = \frac{\boldsymbol{f^{+}(r) + f^{-}(r)}}{\boldsymbol{2}} = \frac{\boldsymbol{\rho_{N+1}(r) - \rho_{N-1}(r)}}{\boldsymbol{2}} \approx \frac{\boldsymbol{\rho^{HOMO}(r) + \rho^{LUMO}(r)}}{\boldsymbol{2}} \quad (5)$$

When a molecule accepts electrons, the electrons tend to go to places where $\boldsymbol{f^{+}(r)}$ is large because it is at these locations that the molecule is most able to stabilize additional electrons. Therefore a molecule is susceptible to nucleophilic attack at sites where $\boldsymbol{f^{+}(r)}$ is large. Similarly, a molecule is susceptible to electrophilic attack at sites where $\boldsymbol{f^{-}(r)}$ is large, this is because these are the regions where electron removal destabilizes the molecule the least.

Therefore, as porphyrin has stronger EDGs, there is a larger value of $f^-(r)$ at EDGs which lose electrons easier.

Fukui function is a real space function, which is commonly studied by means of visualization of iso surface. In order to achieve quantitative comparison between different sites, one can calculate Condensed Fukui Function based on atomic charges. In the condensed version, atomic population number is used to represent the amount of electron density distribution around an atom. The definition of condensed Fukui function for an atom, say A, can be written as: [19]

Nucleophilic attack: $f_A^+ = q_N^A - q_{N+1}^A$ (6)

Electrophilic attack: $f_A^- = q_{N-1}^A - q_N^A$ (7)

Radical attack: $f_A^0 = (q_{N-1}^A - q_{N+1}^A)/2$ (8)

Specifically, q^A is the atomic charge. We adopted a widely used population method (Hirshfeld Population analysis) to evaluate the atomic charges using software Multiwfn 3.3.6. The advantages of the Hirshfeld population are evident, whose applicability is not constrained by the type of wave function and is insensitive to the quality of wave function. Besides, the atom-condensed Hirshfeld Fukui functions tend to be nonnegative. Olah[20] illustrated how Hirshfeld charge is successfully used to study the reactive site by means of condensed Fukui function.

Furthermore, we extended the definition of condensed Fukui for an atom (say A) to a functional group (say M), which is written as:

Nucleophilic attack: $f_M^+ = \sum_A f_A^+ = \sum_A (q_N^A - q_{N+1}^A)$ (9)

Electrophilic attack: $f_M^- = \sum_A f_A^- = \sum_A (q_{N-1}^A - q_N^A)$ (10)

Radical attack: $f_M^0 = \sum_A f_A^0 = \sum_A (q_{N-1}^A - q_{N+1}^A)/2$ (11)

2.4 Charge Transfer Dipole moment (μ_{CT})

Tangui Le Bahers[21] proposed a method for analyzing charge-transfer (CT) during electron transition. The electron density variation between excited state (EX) and ground state (GS) is:

$$\Delta\rho(r) = \rho_{EX}(r) - \rho_{GS}(r) \quad (12)$$

It should be noticed that the geometry used in calculating $\rho_{EX}(r)$ and $\rho_{GS}(r)$ must be identical, otherwise the resulting $\Delta\rho(r)$ is meaningless. The $\Delta\rho(r)$ can be devided into positive and negative parts, namely $\rho_+(r)$ and $\rho_-(r)$. Of course, the integral of $\rho_+(r)$ and $\rho_-(r)$ should be equal, and if evident inequality is observed, that means the error in numerical integral is unneglectable, and denser grid is required. Even though what was analyzed is single-electron excitation, the magnitude of $\rho_+(r)$ and $\rho_-(r)$ as well as their integrals can also be theoretically larger than 1.0 as the excitation of an electron leads to a distribution reorganization of the remaining electrons, which also contribute to $\Delta\rho(r)$. [22]

The transferred charge q_{CT} is the magnitude of the integral of $\rho_+(r)$ and $\rho_-(r)$. The barycenters of positive and negative parts can be computed as

$$R_+ = \int r\rho_+(r)dr \;/\; \int \rho_+(r)dr \quad (13)$$

$$R_- = \int r\rho_-(r)dr \;/\; \int \rho_-(r)dr \quad (14)$$

The component coordinates of R_+ will be referred to as X_+, Y_+, Z_+, and of R- as X_-, Y_-, Z_-. The distance between the two barycenters dertermines the CT length.

$$D_{CT,X} = |X_+ - X_-| \qquad D_{CT,Y} = |Y_+ - Y_-| \qquad D_{CT,Z} = |Z_+ - Z_-| \quad (15)$$

The dipole moment variation caused by CT is evaluated as

$$\mu_{CT,X} = (X_+ - X_-)q_{CT}, \qquad \mu_{CT,Y} = (Y_+ - Y_-)q_{CT},$$
$$\mu_{CT,Z} = (Z_+ - Z_-)q_{CT} \quad (16)$$

2.5 Computational details

All ground state (GS) molecules were optimized using B3LYP function with 6-31g (d, p) basis set. With the identical geometries, we calculated the excited states (EXs) using BP86 function with 6-31+g(d, p) basis set, since the hybrid method B3LYP always overestimates the transition energy according to the literature,[23] and BP86 is well consistent with the experimental results.[23] Conductor-like polarizable continuum model(C-PCM) is used to simulate the environment of ethanol when conducting GS and EX calculations. [24]

To prove reliability, Perdew-Burke-Ernzerhof exchange-correlation (PBE0), CAM-B3LYP and LC-wPBE for long range exchange-correlation[24] are also employed to calculate the ground states of molecules **DPA**, **IDB**, **ISB** for comparison with the "more suitable function" B3LYP and experimental results. As for the reliability of excited state computation, we compared the computed transitions with the absorption peak in experimental UV-Vis absorption spectra as another diagnostic tool.[25]

All the above calculations are performed using Gaussian 09 software package.[26] The calculations concerning Fukui Function, Condensed Fukui Function and charge transfer indexes were performed using Multiwfn software. [19, 27]

3. Results and discussion

3.1 Analysis of the reliability of computed results

The first step in the calculations is to get the correct ground geometries of the dyes. Three molecules (**DPA**, **IDB** and **ISB**), which have been synthesized and examined previously, are employed to evaluate the computation method. It is found that B3LYP is more suitable than PBE0, CAM-B3LYP and LC-wPBE for computation by comparing the calculated HOMOs and LUMOs with experimental values (Table 1). It is clear that the calculated HOMOs and LUMOs using B3LYP are closer to the experimental results than using other functions.

To determine the reliability of BP86 functions for the excited state calculations, molecules **DPA**, **IDB** and **ISB** are again employed as examples. From Table 2, it can be observed that there is an acceptable difference of less than 20 nm when comparing the calculated absorption peaks with experimental values. Figure 3 shows that the experimental UV-Vis absorption spectra almost coincide with the calculated excited states. Therefore, BP86 functions are employed to calculate all excited states of the newly designed molecules.

Table 2 Comparison of absorption peaks (nm) of **DPA**, **IDB** and **ISB**

Molecules	Exp	BP86
DPA	432.8	434.900
IDB	426.6	441.840
ISB	424.2	443.330

PCCP

Paper

Table 1 Comparisons of the calculated HOMOs and LUMOs with experimental results for **DPA**, **IDB** and **ISB**, with all values in eV and calculated using 6-31g (d, p) basis set and C-PCM solvent model (solvent=ethanol)

Molecules		Exp	B3LYP	CAM-B3LYP	PBE0	lc-wPBE
DPA	LUMO	-3.117	-2.740	-1.706	-2.706	-1.152
	HOMO	-5.101	-5.044	-6.100	-5.282	-7.135
IDB	LUMO	-3.079	-2.742	-1.713	-2.711	-1.154
	HOMO	-5.135	-5.095	-6.171	-5.341	-7.192
ISB	LUMO	-3.144	-2.758	-1.733	-2.734	-1.168
	HOMO	-5.214	-5.233	-6.242	-5.490	-7.260

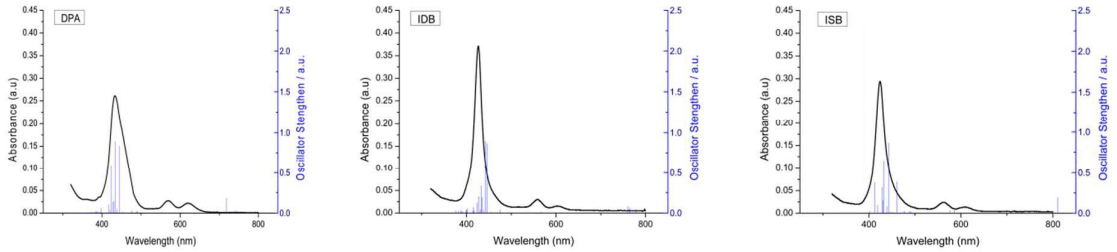

Figure 3 Experimental UV-Vis absorption spectra (Black line) and calculated vertical electronic transitions (Blue bars) of **DPA**, **IDB** and **ISB**, TD-DFT calculations using BP86 function with 6-31+g (d, p) basis set and CPCM solvent model (solvent=ethanol)

3.2 Porphyrin with different electron-donating groups (D)—DPA, IDB, ISB

According to our experimental efficiency (η) results[15] of **DPA**-, **IDB**- and **ISB**-sensitized solar cells, **IDB** (5.26%) is higher than **DPA** (4.05%) and **ISB** is the lowest (2.62%). So are the J_{sc} and V_{oc} values, i.e. **IDB** (9.68 mA cm^{-2}, 740 mV) is larger than **DPA** (7.45 mA cm^{-2}, 730 mV), and **ISB** is the smallest (6.43mA cm^{-2}, 660 mV).

The different cell performance should be caused by the different diarylamino groups. In order to analyze and compare their electron-donating abilities, the Fukui Function and extensive condensed Fukui function of different diarylamino groups (f_M^-) were calculated. Figure 4 is the visualization of Fukui Function. The extended condensed Fukui Function (f_M^-) is calculated to be 0.3709, 0.4765 and 0.1396 for **DPA**, **IDB** and **ISB**, respectively. It can be seen that iminodibenzyl is the strongest electron-donating group with the largest f_M^- and iminostilbene is the weakest. The different electron-donating abilities of the diarylamino group can have a significant influence on charge transfer.

Table 4 shows that charge transfer distance (D_{CT}), transferred charge (q_{CT}), and dipole moment variation (μ_{CT}) increase in the order **ISB**<**DPA**<**IDB**. Thus, on the basis of Tangui Le Bahers' model,[15] the electron lifetime (τ_e) is to increase in the order **ISB**<**DPA**<**IDB**. As a result, **IDB** has a more efficient charge transfer which contributes to the greater values of J_{sc} and V_{oc} of **IDB**-sensitized cell compared to those of **ISB**- and **DPA**-based cells with **ISB** showing the worst cell performance. Overall, it is believed that the strong electron-donating ability of the iminodibenzyl group facilitates CT of **IDB** and boosts its cell performance significantly.

Table 3 Experimental results[15] of **DPA**, **IDB** and **ISB**

	J_{SC}/mA cm^{-2}	V_{OC}/mV	FF (%)	η (%)
DPA	7.45	730	74.47	4.05
IDB	9.68	740	73.48	5.26
ISB	6.43	660	61.73	2.62

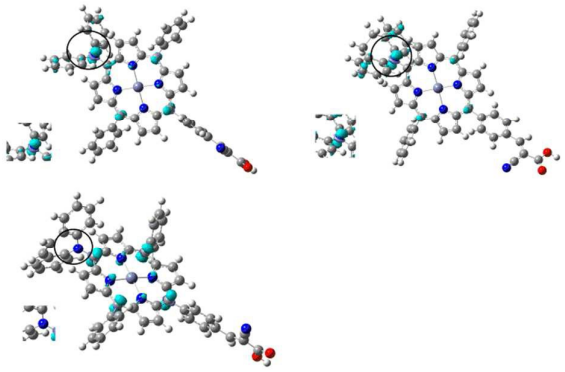

Figure 4 Visualization of Fukui Function for **DPA**, **IDB**, and **ISB** (isovalue 0.02a.u., density 0.003)

Table 4 Computed charge transfer distance (D_{CT}), transferred charge (q_{CT}), and dipole moment variation (μ_{CT}) (Medium quality grid, about 512000 points in total)

	D_{CT}	μ_{CT}	qCT	
	/ Bohr	/ a.u.	positive parts	negative parts
DPA	0.331	0.368	1.113	-1.125
IDB	0.386	0.436	1.13	-1.137
ISB	0.204	0.233	1.141	-1.133

3.3 A series of newly designed Porphyrin with different electron-donating groups (D)— Dye1-Dye6

To further evaluate the reliability of the method of the extended condensed Fukui Function in predicting the photovoltaic properties of the sensitizers, a series of new structure based on porphyrin **IDB** were designed (Figure 2). The electron-donating abilities of the iminodibenzyl vary significantly by introducing different EDGs or EWGs to the two benzo rings of the iminodibenzyl substituent para to the amino atom as shown in Figure 2. By theoretical calculation, correlation between the extended condensed Fukui Function values of the newly designed porphyrins with their calculated photovoltaic properties such as the CT parameters like μ_{CT} as mentioned above can be established. Furthermore, the molecule which should potentially lead to the best cell performance can be determined. The methodology based on the theoretical calculation developed here should provide a valuable guide for the experimental synthesis and future molecular design for a high performance sensitizer.

3.4 Extended Fukui Function of donors (Dye1-Dye6)

Table 5 shows the results of the extended condensed Fukui Function(f_M^-) of different iminodibenzyl substituents in molecules **Dye1**-**Dye6**. It is clear that the electron-donating abilities of the iminodibenzyl substituent decrease in the order **Dye1**>**Dye2**>**Dye3**>**Dye4**>**IDB**>≈**Dye5**>**Dye6**. Thus, among the newly designed molecules, **Dye1** and **Dye2** have EDGs with strongest electron-donating ability, while porphyrins **Dye3** and **Dye4** contain relatively stronger donors than **IDB**. On the contrast, the donor of **Dye6** has relatively weaker electron-donating ability than **IDB**. Compared to the hydrogen in **IDB**, it can be seen that the results are in accord with the electron-donating/electron-withdrawing abilities of the introduced substituent among the newly designed porphyrins except for **Dye5**. Interestingly, for **Dye5** with two strong electron-drawing fluorine atoms introduced to the benzo rings of the iminodibenzyl group in the porphyrin IDB, the extended condensed Fukui Function(f_M^-) remains almost unchanged (0.4743 for **Dye5** Vs 0.4765 for **IDB**). This actually can be attributed to the p-π conjugated effect[28] due to the presence of the electron lone pairs outside the fluorine atom, which weakens the electron-withdrawing abilities of fluorine.

Table 5 Extended condensed Fukui Function of **Dye1**-**Dye6** and **IDB** （using Hirshfeld Population analysis）

	Dye 1	**Dye 2**	**Dye 3**	**Dye 4**	**Dye 5**	**Dye 6**	**IDB**
Extensive Condensed Fukui Function	0.8436	0.8101	0.6780	0.5678	0.4743	0.3051	0.4765

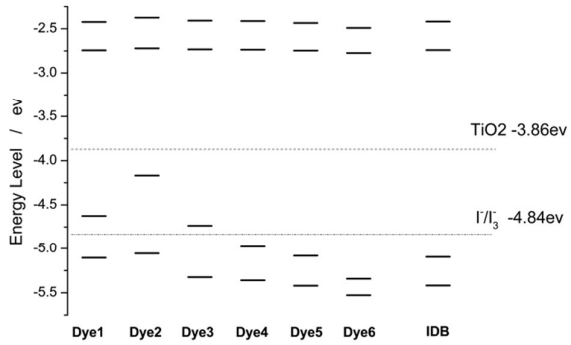

Figure 5 The calculated energy level alignments of **Dye1**-**Dye6** and IDB, using B3LYP function with 6-31g (d, p) basis set and C-PCM solvent model (solvent=ethanol)

3.5 Frontier Molecule Orbital Theory and analysis of energy level (Dye1-Dye6)

Surprisingly, it is found that based on the calculated energy level alignments shown in Figure 5, the HOMO energy levels of porphyrins **Dye1**, **Dye2** and **Dye3** lie above the redox potential of the redox couple (I^- / I_3^-). Thus, it can be determined that **Dye1**, **Dye2** and **Dye3** are not suitable to be used in DSSCs. The corresponding photo-oxidized dyes cannot be reduced by the redox couple to their ground states. **Dye4**-**Dye6** have valid energy level alignment. More specifically, **Dye4** has a smaller HOMO-LUMO gap than **IDB** which should facilitate sunlight absorption by red-shifting light absorption and be beneficial for the enhancement of efficiency (η).

The above results suggested that the additional EDG can have a critical influence on the HOMO energy levels of the D-π-A, which will determine the driving force for the regeneration of the oxidized dye molecules by the redox couple. Namely, the extremely strong EDG will make the HOMO of a dye lie above the potential of the redox couple which makes the regeneration of an oxidized dye thermodynamically unfavorable, resulting in a failed circuit current. On the precondition of obtaining valid alignment of energy level, which means the regeneration of an oxidized dye molecule is thermodynamically feasible, a stronger EDG is conducive to narrow

HOMO-LUMO gap and should harvest more sunlight energy.

3.6 Charge Transfer Dipole moment (μ_{CT}) of Dye4-Dye6

Next, to correlate the Fukui function value with the photovoltaic properties of the molecules, we analyzed CT during electron transition occurring in valid molecules **Dye4**-**Dye6**. Among the three CT indexes ($D_{CT,}$ q_{CT} and μ_{CT}), CT dipole moment is the most important index which is the product of D_{CT} and q_{CT}. Table 6 shows that μ_{CT} decreases in the order **Dye4**>**IDB**>**Dye5**>**Dye6**. Thus on the basis of Tangui Le Bahers'[21] model, the electron lifetime (τ_e) will also decrease in the order **Dye4**>**IDB**>**Dye5**>**Dye6**. The results suggested that porphyrin **Dye4** may have a more efficient charge transfer than **IDB** leading to a better cell performance due to the stronger electron-donor present in **Dye4**.

Table 6 Computed charge transfer distance (D_{CT}), transferred charge (q_{CT}), and dipole moment variation (μ_{CT}) (Medium quality grid of 512000 points in total)

	D_{CT}	μ_{CT}	qCT	
	/ Bohr	/ a.u.	positive parts	negative parts
Dye4	0.289	0.509	1.758	-1.741
Dye5	0.212	0.360	1.698	-1.702
Dye6	0.120	0.204	1.698	-1.677
IDB	0.386	0.436	1.130	-1.137

4. Conclusions

The correlation between the electron donating abilities of the derived iminodibenzyl group and CT was built to evaluate the cell performance on the basis of **Dye1**-**Dye6**. The porphyrins bearing extremely strong EDGs like **Dye1**-**Dye3** are not suitable to be used as sensitizers in DSSCs because they would fail in the generation of photocurrent due to the higher level of the HOMO energy than the redox potential of the redox couple (I^- / I_3^-). The one with a medium EDG (**Dye4**) has a valid energy level alignment with a smaller HOMO-LUMO gap than porphyrin **IDB** with an unsubstituted iminodibenzyl group, resulting in a better CT computation result. Therefore **Dye4** is expected to show better photovoltaic performance than **IDB**. Our theoretical studies demonstrate that Fukui Function and extended condensed Fukui Function are in accord with the electron-donating abilities of EDGs. The Tangui Le Bahers' model can be adopted to analyze porphyrins' CT during electron transition. In summary, the reliable method involving the employment of Fukui Function extended condensed Fukui Function and Tangui Le Bahers' model can be used for screening D-π-A type porphyrin sensitizers for use in DSSCs and as guidance for the future molecular design.

Acknowledgements

Project is supported by the National Natural Science Foundation of China (No. 21476162) and the National International S&T Cooperation Foundation of China (No. 2012DFG41980). Assistance with High Performance Computing Center of Tianjin University is appreciated.

References

1. B. O'Regan and M. Gratzel, *Nature*, 1991, **353**, 737-740.
2. A. Hagfeldt, G. Boschloo, L. Sun, L. Kloo and H. Pettersson, *Chem. Rev.*, 2010, **110**, 6595-6663.
3. K. D. Seo, M. J. Lee, H. M. Song, H. S. Kang and H. K. Kim, *Dyes Pigments*, 2012, **94**, 143-149.
4. M. Gouterman, in *The Porphyrins*, ed. D. Dolphin, Academic Press, New York, 1978, vol. 3, Part A, pp. 1-165.
5. S. Hayashi, M. Tanaka, H. Hayashi, S. Eu, T. Umeyama, Y. Matano, Y. Araki and H. Imahori, *J. Phys. Chem. C*, 2008, **112**, 15576-15585.
6. T. Le Bahers, T. Pauporte, P. P. Laine, F. Labat, C. Adamo and I. Ciofini, *J. Phys. Chem. Lett.*, 2013, **4**, 1044-1050.
7. C. Chitpakdee, S. Namuangruk, K. Suttisintong, S. Jungsuttiwong, T. Keawin, T. Sudyoadsuk, K. Sirithip, V. Promarak and N. Kungwan, *Dyes Pigments*, 2015, **118**, 64-75.
8. Y. Wang, B. Chen, W. Wu, X. Li, W. Zhu, H. Tian and Y. Xie, *Angew. Chem. Int. Edit*, 2014, **53**, 10779-10783.
9. X. Sun, Y. Wang, X. Li, H. Agren, W. Zhu, H. Tian and Y. Xie, *Chem. Commun.*, 2014, **50**, 15609-15612.
10. S. Mathew, A. Yella, P. Gao, R. Humphry-Baker, B. F. Curchod, N. Ashari-Astani, I. Tavernelli, U. Rothlisberger, M. K. Nazeeruddin and M. Gratzel, *Nat. Chem.*, 2014, **6**, 242-247.
11. K. Kakiage, Y. Aoyama, T. Yano, K. Oya, J.-i. Fujisawa and M. Hanaya, *Chem. Commun.*, 2015, DOI: 10.1039/C5CC06759F.
12. M. Urbani, M. Grätzel, M. K. Nazeeruddin and T. Torres, *Chem. Rev.*, 2014, **114**, 12330-12396.
13. B. Liu, W. Zhu, Y. Wang, W. Wu, X. Li, B. Chen, Y.-T. Long and Y. Xie, *J. Mater. Chem.*, 2012, **22**, 7434-7444.
14. T. Wei, X. Sun, X. Li, H. Ågren and Y. Xie, *ACS. Appl. Mater. Inter.*, 2015, **7**, 21956-21965.
15. Y. Liang, X. Xue, W. Zhang, C. Fan, Y. Li, B. Zhang and Y. Feng, *Dyes Pigments*, 2015, **115**, 7-16.
16. K. Fukui, *Accounts. Chem. Res.*, 1981, **14**, 363-368.
17. R. G. Parr and W. Yang, *J. Am. Chem. Soc.*, 1984, **106**, 4049-4050.
18. W. Y. Paul W. Ayers and a. L. J. Bartolotti, in *Chemical Reactivity Theory: A Density Functional View*, ed. P. K. Chattaraj, CRC Press, New York, 2009, ch. 18, pp. 255-267.
19. W. Yang and W. J. Mortier, *J. Am. Chem. Soc.*, 1986, **108**, 5708-5711.
20. J. Oláh, C. Van Alsenoy and A. B. Sannigrahi, *J. Phys. Chem. A*, 2002, **106**, 3885-3890.
21. T. Le Bahers, C. Adamo and I. Ciofini, *J. Chem. Theory. Comput*, 2011, **7**, 2498-2506.
22. T. Lu and F. Chen, *J. Chem. Theory. Comput*, 2012, **33**, 580-592.
23. G. A. Peralta, M. Seth, H. Zhekova and T. Ziegler, *Inorg. Chem.*, 2008, **47**, 4185-4198.
24. X. Gu and Q. Sun, *Phys. Chem. Chem. Phys.*, 2013, **15**, 15434-15440.
25. N. M. O'Boyle, A. L. Tenderholt and K. M. Langner, *J. Comput. Chem.*, 2008, **29**, 839-845.

26. G. W. T. M. J. Frisch, H. B. Schlegel, G. E. Scuseria, M. A. Robb, J. R. Cheeseman, G. Scalmani, V. Barone, B. Mennucci, G. A. Petersson, H. Nakatsuji, M. Caricato, X. Li, H. P. Hratchian, A. F. Izmaylov, J. Bloino, G. Zheng, J. L. Sonnenberg, M. Hada, M. Ehara, K. Toyota, R. Fukuda, J. Hasegawa, M. Ishida, T. Nakajima, Y. Honda, O. Kitao, H. Nakai, T. Vreven, J. A. Montgomery, Jr., J. E. Peralta, F. Ogliaro, M. Bearpark, J. J. Heyd, E. Brothers, K. N. Kudin, V. N. Staroverov, T. Keith, R. Kobayashi, J. Normand, K. Raghavachari, A. Rendell, J. C. Burant, S. S. Iyengar, J. Tomasi, M. Cossi, N. Rega, J. M. Millam, M. Klene, J. E. Knox, J. B. Cross, V. Bakken, C. Adamo, J. Jaramillo, R. Gomperts, R. E. Stratmann, O. Yazyev, A. J. Austin, R. Cammi, C. Pomelli, J. W. Ochterski, R. L. Martin, K. Morokuma, V. G. Zakrzewski, G. A. Voth, P. Salvador, J. J. Dannenberg, S. Dapprich, A. D. Daniels, O. Farkas, J. B. Foresman, J. V. Ortiz, J. Cioslowski, D. J. Fox. Gaussian 09 (Revision D.01); Gaussian Inc.: Wallingford CT, 2013.

27. T. Lu and F. Chen, *J. Mol. Graph. Model.*, 2012, **38**, 314-323.

28. C. A. Hollingsworth, P. G. Seybold and C. M. Hadad, *Int. J. Quantum. Chem.*, 2002, **90**, 1396-1403.